

# The Effect of Acid Activation on Some Physicochemical Properties of a Bentonite

Müşerref ÖNAL, Yüksel SARIKAYA, Tülay ALEMDAROĞLU

*Ankara University, Faculty of Science, Department of Chemistry  
06100 Tandoğan, Ankara-TURKEY*

İhsan BOZDOĞAN

*Eczacıbaşı Ceramic Industry, Kısıklı Cad. 1, Altunizade,  
81190 Üsküdar, İstanbul-TURKEY*

Received 19.03.2001

A white calcium bentonite (CaB) from the Kütahya region/Turkey was activated by heating it for 6 hours at 97°C in H<sub>2</sub>SO<sub>4</sub> solution. The mass percentage of H<sub>2</sub>SO<sub>4</sub> in the bentonite-acid mixture was varied from 0 to 70%. The chemical analysis (CA), cation exchange capacity (CEC), differential thermal analysis (DTA) curves and X-ray diffraction (XRD) patterns of the prepared samples were determined. The specific surface area (A) and the specific micropore-mesopore volume (V) were calculated respectively from the adsorption and desorption data of N<sub>2</sub> obtained at liquid N<sub>2</sub> temperature. How the calcium montmorillonite (CaM) layers in the CaB were decomposed during the preservation of the crystal structure is discussed by using CA, CEC, DTA and XRD data. The variations in the porosity of CaB during acid activation were related to the variations in the crystal structure and are discussed. Although the values of A and V were 43 m<sup>2</sup>g<sup>-1</sup> and 0.107cm<sup>3</sup>g<sup>-1</sup> respectively for the original bentonite, these values reached a maximum and were 134 m<sup>2</sup>g<sup>-1</sup> and 0.295 cm<sup>3</sup>g<sup>-1</sup> respectively after activation by 40% H<sub>2</sub>SO<sub>4</sub>.

**Key Words:** Acid Activation, Bentonite, Cation Exchange Capacity, Pore Volume, Surface Area.

## Introduction

Clays whose basic clay mineral is montmorillonite, or smectite, are generally called bentonites. Bentonites, which are employed in more than 25 different areas, are among the most important industrial raw materials<sup>1</sup>. The chemical and mineralogical structures of the bentonites, which are activated by heating in strong acids, undergo considerable transformations<sup>2-4</sup>. Acid activated bentonites are used as adsorbents in the bleaching of edible oils<sup>5</sup>, in the production of carbonless copy paper<sup>6</sup>, and in the preparation of pillared clays<sup>7</sup>, organoclays<sup>8</sup> and heterogeneous catalysts<sup>9-12</sup>.

The surface acidity and the porous structure of bentonites can be changed to the desired extent by acid activation<sup>13-15</sup>. These changes depend on the smectite minerals, other clay minerals and non-clay minerals contained in the bentonite as well as the chemical composition, the type of cations between the layers, the

type of the acid, the mass percent of the acid in the bentonite-acid mixture, the process temperature and the process period.

As in most solids, there are three types of pores in bentonites. Empty spaces in a solid that are smaller than 2nm are called micropores, those between 2nm and 50nm are called mesopores and those larger than 50nm are called macropores. Although the micropores and mesopores lie within the particles, the macropores lie between the particles.

Smectites are among the most important solids that contain natural mesopores. They also contain a small amount of micropores. The large amounts of smectite minerals contained in the bentonites are the main sources of porosity. The physicochemical properties of bentonites such as adsorption, bleaching and catalytical activity depend extensively on the micro- and mesopores. The effect of macropores on these properties is negligible. In the investigation of porous structure, different procedures such as N<sub>2</sub>-adsorption, Hg-porosimetry and thermoporometry are used<sup>16–17</sup>.

The first aim of this study was to investigate and discuss the variation of some of the physicochemical properties, such as chemical composition, cation exchange capacity (CEC), mineralogical destruction, specific surface area and specific micropore-mesopore volume, of a bentonite from the Kütahya region (Turkey) by sulphuric acid activation. The second aim was to determine the degree of correlation between the relative crystallinities obtained from the normalization of the dehydroxylation peaks of the differential thermal analysis (DTA) curves and the normalization of the 001 peaks of the X-ray diffraction (XRD) patterns of the montmorillonite mineral.

## Materials and Methods

White calcium bentonite (CaB) from the beds in the Kütahya region (Turkey) whose basic clay mineral is calcium montmorillonite (CaM), was used in the experiments. CaB produces a mud of high plasticity and is therefore used as a binder in porcelain production. The location map of this bentonite and the variations in some of its rheological properties by Na<sub>2</sub>CO<sub>3</sub> activation have been given in two previous articles<sup>18,19</sup>. The variation of some of the physicochemical properties by the thermal treatment temperature of the same bentonite was also investigated<sup>20</sup>.

Analytically pure H<sub>2</sub>SO<sub>4</sub> (98%) and methylene blue were supplied by Merck Chemical Company.

CaB was first ground and then dried at 105°C for 4 hours. Eight samples, each having a mass of 20g, were taken from the dried CaB. The first sample was mixed with 400mL of water and a suspension was prepared. Other samples were mixed with 400mL of H<sub>2</sub>SO<sub>4</sub> solutions which had different concentrations, such that the mass percentage of the H<sub>2</sub>SO<sub>4</sub> in the bentonite-acid mixture would be 10, 20, 30, 40, 50, 60 and 70% respectively. Thus, 7 other different suspensions were prepared. The acid activation was performed by heating a total of 8 suspensions in a shaking water bath at 97°C. The activated samples were filtered under vacuum and the precipitate was washed with distilled water until it was free of SO<sub>4</sub><sup>2-</sup> ions. The samples, which were then dried for 24 hours at 105°C, were labeled K00, K10, ..., K70 and were stored in polyethylene bags to be used later in the experiments.

The mass fractions of particles smaller than 2.7µm in each sample were determined by an Andreasen pipette<sup>21</sup>.

The decrease in mass of the samples, which were heated for 2 hours at 1000°C, was recorded as the loss on ignition (LOI). A complete chemical analysis of the K00 sample was performed. For the other samples,

only the  $R_xO_y$  ( $Al_2O_3+Fe_2O_3+MgO$ ) mass percents ( $R_xO_y\%$ ) were determined. The chemical analysis was performed with an atomic absorption spectrophotometer, Hitachi Z-8200.

The CECs, defined as the milliequivalents of exchangeable cations contained in 100g of clays or clay minerals, were determined by the methylene blue standard procedure<sup>22</sup>.

The DTA curves of all the samples were obtained by a Netzsch Simultaneous TG-DTG-DTA Instrument Model 429 at a heating rate of  $20Kmin^{-1}$ , and  $\alpha-Al_2O_3$  was used as an inert material.

The XRD patterns of all the samples were determined by a Phillips PW 1730 powder diffractometer with a Ni filter and  $CuK_{\alpha}$  X-rays having 0.15418 nm wavelength.

The adsorption and desorption of  $N_2$  at liquid  $N_2$  temperature was performed by a volumetric instrument fully constructed of Pyrex glass<sup>23</sup>. The relative equilibrium pressures ( $p/p^0$ ) were determined by taking the ratio of the equilibrium pressures ( $p$ ) during the adsorption and desorption to the vapor pressure ( $p^0$ ) of liquid  $N_2$  at the place of the experiment.

## Results and Discussion

### Particle Size

Most clay particles are smaller than  $2\mu m$ . In the bentonite chosen as the material of this study, the mass fraction of the particles was smaller than  $2.7\mu m$ , decreasing as the  $H_2SO_4\%$  in the bentonite-acid mixture increased, as shown in Figure 1. According to this trend, particles lose their clay mineral property as the acid activation progresses.

### Chemical Analysis

The chemical analysis of the original CaB (K00), presented in "mass %", was determined as follows:  $SiO_2$ , 72.08;  $Al_2O_3$ , 14.40;  $Fe_2O_3$ , 0.78;  $TiO$ , 0.08;  $CaO$ , 2.15;  $MgO$ , 1.63;  $Na_2O$ , 0.43;  $K_2O$ , 1.05 and LOI, 7.35. The presence of  $K_2O$  showed that CaB contained some illite (I).

The decrease in the  $R_xO_y\%$  that was left in the CaM(2:1) layers after activation by  $H_2SO_4\%$  in the bentonite-acid mixture is shown in Figure 2. The interpretation of the results represented in this figure may be as follows: As the  $H_2SO_4\%$  increases between 0 and 10, the exchangeable cations between the 2:1 layers leave first, and are replaced by the  $H^+$  ions. Since only a small quantity of  $Mg^{2+}$ ,  $Fe^{3+}$  and  $Al^{3+}$  leaves the 2:1 layers, the change in the  $R_xO_y\%$  is small. As the  $H_2SO_4\%$  increases between 10 and 50% , the cations  $Mg^{2+}$ ,  $Fe^{3+}$  and  $Al^{3+}$  dissolve easily from the 2:1 layers, so the decrease in  $R_xO_y\%$  is great<sup>24</sup>. As the  $H_2SO_4\%$  increases between 50 and 70% , because of the decreased amounts of  $Mg^{2+}$ ,  $Fe^{3+}$  and  $Al^{3+}$  in the 2:1 layers and the difficult dissolution of  $Al^{3+}$  (which can be maximum 15%) in the tetrahedron sheets of the I (2:1) layers<sup>25</sup>, the decrease in the  $R_xO_y\%$  is small.

### CEC Values

The CEC of the original CaB and of the CaM that was obtained by its purification were respectively determined as 52 and 68 meq  $(100g)^{-1}$ . Because of the existence of the non-clay minerals whose CECs are close to zero in CaB, the CEC of CaB is smaller than that of CaM. By assuming that the CEC originates only from the CaM, the mass percent of the CaM in CaB can be calculated as follows:  $(52/68) \times 100 = 76\%$ .

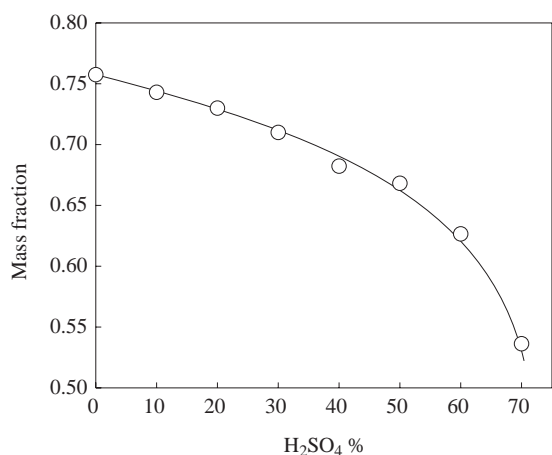


**Figure 1.** The variation of the mass fraction of particles whose sizes are smaller than  $2.7\mu\text{m}$  in the bentonite by the mass percent of  $\text{H}_2\text{SO}_4$  in the bentonite-acid mixture.

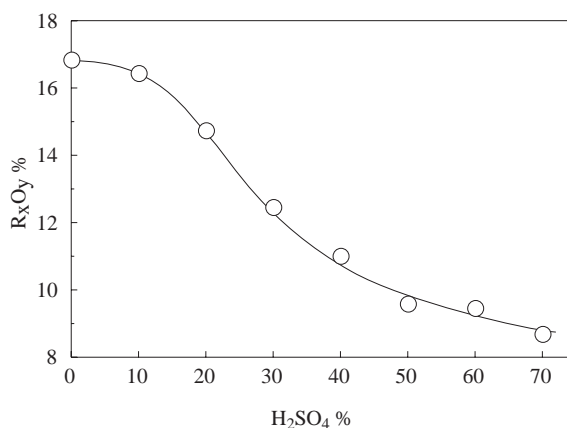


**Figure 2.** The variation of the mass percent of  $\text{R}_x\text{O}_y(\text{Al}_2\text{O}_3 + \text{Fe}_2\text{O}_3 + \text{MgO})$  that was left in the bentonite after the acid activation, by the mass percent of  $\text{H}_2\text{SO}_4$  in the bentonite-acid mixture.

The variation of the CEC by the  $\text{R}_x\text{O}_y\%$  is represented in Figure 3. The interpretation of these results is as follows: As the  $\text{R}_x\text{O}_y\%$  decreases by progressing activation, the CEC also decreases linearly. The disappearance of some of the octahedrons whose  $\text{Mg}^{2+}$  cations in their centers were dissolved leads to the disappearance of the excess negative charge originating from them. Similarly, the disappearance of some of the tetrahedrons whose  $\text{Al}^{3+}$  cations in their centers were dissolved leads to the disappearance of the excess negative charge originating from them. In both cases, the unshared electron pairs that appear on oxygens, transform them into hydroxyl groups by taking protons. Hence, the CEC decreases as the  $\text{R}_x\text{O}_y\%$  decreases. When the  $\text{H}_2\text{SO}_4\%$  in the activation increases to 70%, the CEC decreases to 40%. From this result it may be concluded that the CaM layers were 60% decomposed up to this point.

## DTA Curves

The DTA curves of all the samples are represented in Figure 4. The endothermic peaks between 100 and  $250^\circ\text{C}$  of the DTA curves are related to the loss of water from the pores of CaB, i.e. the dehydration. A regular change in the shapes of the dehydration peaks is not observed, since the pore water can be taken in and given out reversibly during the experiments.

The endothermic peaks between 600 and  $750^\circ\text{C}$  of the DTA curves are related to the dehydroxylation, and the exothermic peaks between 950 and  $1050^\circ\text{C}$  are related to the collapse of the crystal structure. It is seen that these peaks become regularly smaller as the activation progresses.

## XRD Patterns

The XRD patterns of all the samples are given in Figure 5. These patterns show that Kütahya bentonite contains CaM as the basic clay mineral, as well as some I as another clay mineral and some opal-CT<sup>26</sup> as a non-clay mineral. The  $d(001)$ -values of CaM and I were found to be 1.50nm and 0.98nm respectively. From the XRD patterns, which are not given in these figures, the  $d(001)$ -values of CaM after it was swollen in ethylene glycol, and after it was heated at  $550^\circ\text{C}$  for one hour were respectively found to be 1.88nm and 0.99nm.

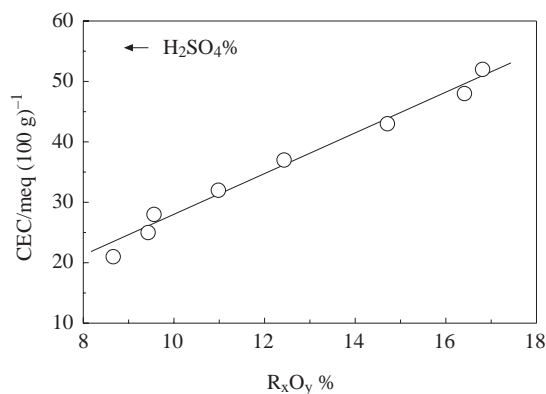


**Figure 3.** The variation of the cation exchange capacity after the acid activation, by the mass percent of  $R_xO_y$  left in the bentonite.

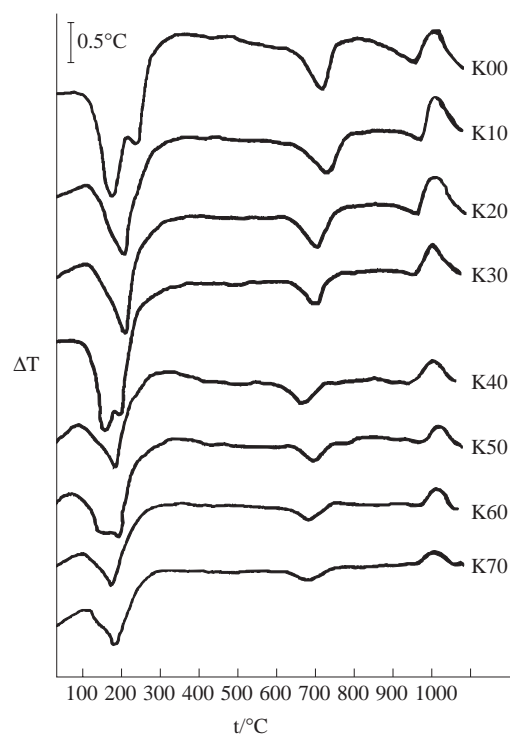


**Figure 4.** The DTA curves of the original and the  $H_2SO_4$  activated bentonites.

As the activation progressed, the position of the peaks of the 001 planes of CaM layers stayed constant, whereas their areas became smaller and smaller. This shows that the CaM decomposes, keeping its  $d(001) = 1.50\text{nm}$  value unchanged. The fact that the 001 peaks of CaM and I were still perceptible, even when the  $H_2SO_4\%$  reached 70, shows that the 2:1 layers were not yet completely decomposed.

### Relative Crystallinity

A normalization can be done by taking the ratio of the peak areas of the DTA and XRD of acid activated samples to the same peak areas of the original sample. The values that are found by the normalization of the dehydroxylation peaks of the DTA curves and the 001 peaks of the XRD patterns are defined as the relative crystallinity (RC). The variation of the RCs obtained from the DTA and XRD, by the  $R_xO_y\%$ , is given in Figure 6. Although the RCs obtained from the two different methods do not coincide, they lie along curves that are not far from each other. The difference between the curves may be due to errors that might have been made in the measurement of peak areas. It can be seen in Figure 2 that when the  $H_2SO_4\%$  in the activation reaches 70% the  $R_xO_y\%$  decreases to 8.7%. It is apparent in Figure 6 that at this point the crystal structure of at least 40% of the 2:1 layers has not yet collapsed. These results are in good correlation with the results of the CA and the CEC.

### The Specific Surface Area (A) and the Specific Pore Volume (A)

By using the data of  $N_2$ -adsorption in the relative pressure interval  $0.05 < p/p^0 < 0.35$  the A values of all the samples were calculated according to the well known Brunauer-Emmett-Teller (BET) procedure<sup>27,28</sup>.

The relative equilibrium pressure at which all of the micropores and mesopores were filled with liquid N<sub>2</sub> was calculated by the corrected Kelvin equation to be 0.96<sup>16</sup>. At this p/p°, the volume of liquid N<sub>2</sub> that remained on one gram of sample was calculated from the desorption data and was taken as the V value<sup>29,30</sup>.

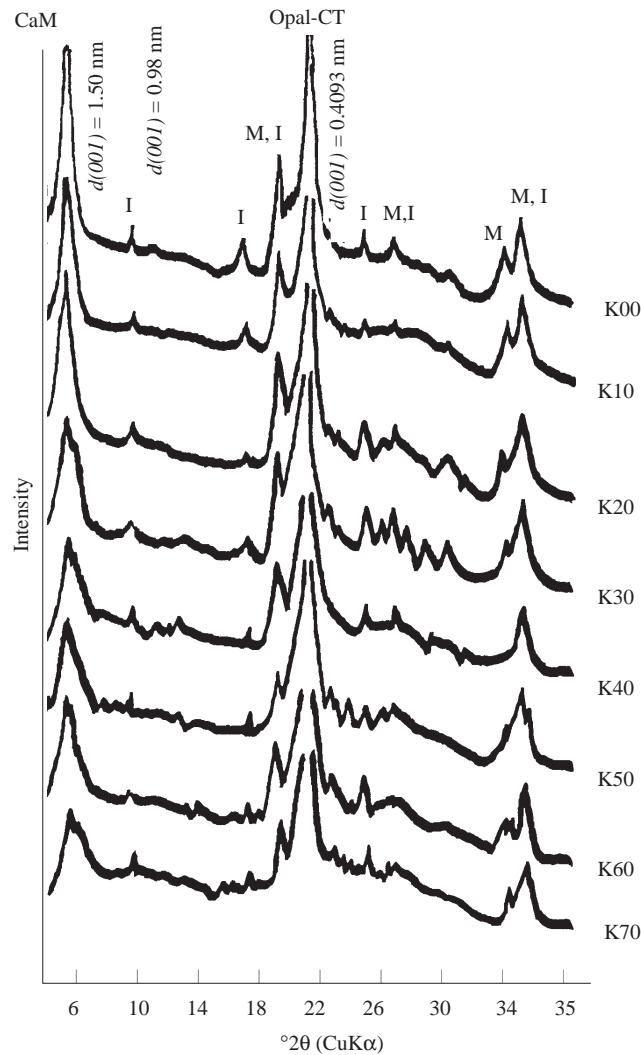


**Figure 5.** The XRD patterns of the original and the H<sub>2</sub>SO<sub>4</sub> activated bentonites (M: montmorillonite, I: illite).

The variation of A and V by R<sub>x</sub>O<sub>y</sub>% is given in Figure 7. As the R<sub>x</sub>O<sub>y</sub>% decreases, i.e. as the activation progresses, A and V increase rapidly at first, reach a maximum and decrease again. At first the rise in A and V is a result of the unoccupied octahedron and tetrahedron spaces remaining from the Mg<sup>2+</sup>, Fe<sup>3+</sup> and Al<sup>3+</sup> ions that have left the 2:1 layers. Then, as the activation progresses, the empty spaces grow larger and the micropores are transformed into mesopores and finally, because of the decomposition of the crystal structure at some locations, some of the mesopores disappear, leading to a drop in A and V. It was shown that by varying the H<sub>2</sub>SO<sub>4</sub>% in the activation between 0 and 70%, it is possible to prepare bentonite samples of different porosities, whose A values lie between 43 and 134 m<sup>2</sup>g<sup>-1</sup> and V values lie between 0.107 and 0.295 cm<sup>3</sup>g<sup>-1</sup>.

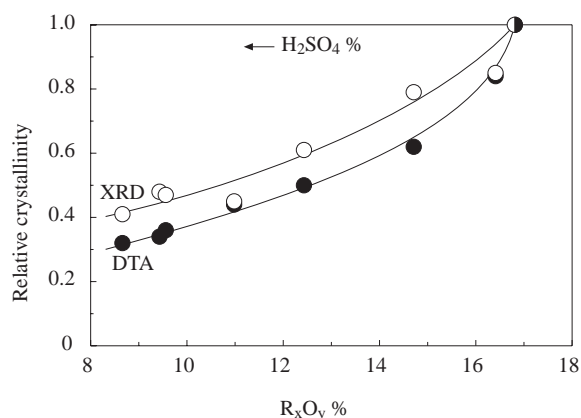


**Figure 6.** The variation of the relative crystallinity defined by the normalization of the dehydroxylation peaks of the DTA curves and of the 001 peaks of the XRD patterns, by the mass percent of  $R_xO_y$  left in the bentonite.

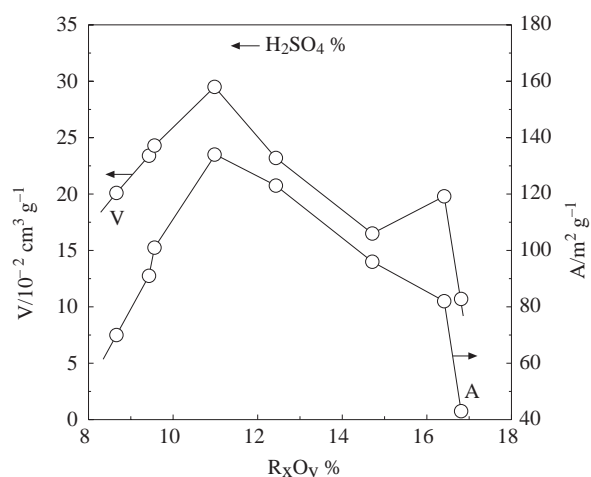


**Figure 7.** The variation of specific surface area and specific pore volume, by the mass percent of  $R_xO_y$  left in the bentonite.

## Conclusions

Important information was obtained about the effect of acid activation on some of the physicochemical properties of bentonites by using CA, CEC, DTA, XRD and  $N_2$  adsorption - desorption data. In addition a numerical approach to the proportion of the destroyed crystal structure was employed by using the RC found by the normalization of the regularly decreasing DTA and XRD peaks. During the acid activation, the partial loss of  $Mg^{2+}$ ,  $Fe^{3+}$  and  $Al^{3+}$  from the 2:1 layers increased the porosity considerably. The  $H_2SO_4$  activation of the investigated bentonite increased three times the A and V values. It was demonstrated that by the acid activation realized at constant temperature and period, it was possible to obtain bentonite samples of required porosity between certain limits by changing only the  $H_2SO_4\%$ .

## Acknowledgments

The authors are grateful to the Ankara University Research Fund for funding this work by the project 96-05-04-02. We are particularly grateful to the Turkish Mineral Research and Exploration Institute, which supplied the bentonite sample, and to Eczacıbaşı Ceramic Industry for their help in our experimental work.

## References

1. H.H. Murray, **Appl. Clay Sci.** **5**, 379-395 (1987).
2. G.A. Mills, J. Holmes and E.B. Cournelius, **J. Phys. Colloid Chem.** **54**, 1170-1185 (1950).
3. R.D. Heyding, R. Ironside, A.R. Norris and R.Y. Pryslazniuk, **Can.J.Chem.** **38**, 1003 - 1016 (1960).
4. P. Komadel, D. Schmidt, J. Madejova and B. Cicel, **Appl. Clay Sci.** **5**, 113 - 122 (1990).
5. E.P. Gonzáles, M.S. Villatrance and A.C. Gallego, **J. Chem. Technol. Biot.** **57**, 213 - 216 (1993).

6. M. Takashima, S. Sano and S. Ohara, J. Imaging, **Sci. Tech.** **37**, 163 - 166 (1993).
7. J.M. Adams, **Appl. Clay Sci.** **2**, 309 - 342 (1978).
8. C. Breen, R. Watson, J. Madejova, P. Komadel and Z. Klapyta, **Langmuir** **13**, 6473 - 6497 (1997).
9. P. Laszlo, **Science** **235**, 1473 - 1477 (1987).
10. T.J. Pinnavaia, **Science** **220**, 365 - 371 (1983).
11. S.R. Chitnis and M.M. Sharma, **React. Funct. Polym.** **32**, 93 - 115 (1997).
12. F. Kooli and W. Jones, **Clay Miner.** **32**, 633 - 644 (1997).
13. N. Javanovic and J. Janackovic, **Appl. Clay Sci.** **6**, 59 - 68 (1991).
14. M.A. Vicente, M. Suárez, J. de D. López - González and M.A. Bañares - Muñoz, **Langmuir** **12**, 566 - 572 (1996).
15. J. Ravichandran and B. Sivasankar, **Clays Clay Miner.** **45**, 854 - 858 (1997).
16. S. Gregg and K.S.W. Sing, **Adsorption, Surface Area and Porosity Academic Press**, London, (1982).
17. Y. Sarıkaya, H. Ceylan, İ. Bozdoğan and M. Akinç, **Turk. J. Chem.** **17**, 119 - 124 (1993).
18. N. Yıldız, Y. Sarıkaya and A. Çalmlı, **Appl. Clay Sci.** **14**, 319 - 327 (1999).
19. N. Yıldız, A. Çalmlı and Y. Sarıkaya, **Turk. J. Chem.** **23**, 309 - (1999).
20. Y. Sarıkaya, M. Önal, B. Baran and T. Alemdaroğlu, **Clays Clay Miner.** **48**, 557 - 562 (2000).
21. F. Patat and K. Kirchner, **Praktikum der Technischen Chemie**, Walter de Gruyter, Berlin, (1968).
22. G. Rytwo, C. Serban, S. Nir and L. Margulies, **Clays Clay Miner.** **39**, 551 - 555 (1991).
23. Y. Sarıkaya and S. Aybar, **Commun. Fac. Sci. Uni. Ank. B24**, 33 - 39 (1978).
24. M.A.R Vicente, M.B. Suárez, J. de D. López-González and M.A. Bañares-Muñoz, **Clays Clay Miner.** **42**, 724 - 730 (1994).
25. I. Takáči, P. Komodel and D. Müller, **Clay Miner.** **29**, 11 - 19 (1994).
26. W.J. Miles, **Anal. Chim. Acta** **286**, 97 - 105 (1994).
27. S. Brunauer, P.H. Emmett and E.J. Teller, **J. Am. Chem.Soc.** **60**, 309 - 319 (1938).
28. M. Önal, Y. Sarıkaya and T. Alemdaroğlu, **Turk. J. Chem.** **25**, 1 - 9 (2001).
29. İ. Sevinç, Y. Sarıkaya and M. Akinç, **Ceram. Int.** **17**, 1 - 4 (1991).
30. Y. Sarıkaya, İ. Sevinç and M. Akinç, **Powder Tech.** **116**, 109 - 114 (2001).